Fluoroscopy of the Elbow

A Cadaveric Study Defining New Standard Projections to Visualize Important Anatomical Landmarks

Sebastian A. Müller, MD, Lars Adolfsson, MD, Cornelia Baum, MD, Magdalena Müller-Gerbl, MD, Andreas M. Müller, MD, and Daniel Rikli, MD

Investigation performed at the University of Basel, Basel, Switzerland, and Linköping University, Linköping, Sweden

Background: Despite new 3-dimensional imaging modalities, 2-dimensional fluoroscopy remains the standard intraoperative imaging modality. The elbow has complex anatomy, and defined standard fluoroscopic projections are lacking. Therefore, the aim of this study was to define standard projections of the elbow for intraoperative fluoroscopy.

Methods: This study consisted of 2 parts. In part I, dissected cadaveric elbows were examined under fluoroscopy, and their radiographic anatomical features were assessed, with focus on projections showing defined anatomical landmarks. In part II, projections from part I were verified on entire cadavers to simulate intraoperative imaging. Standard projections for anteroposterior (AP) and lateral views as well as oblique and axial views were recorded.

Results: Eight standardized projections could be defined and included 3 AP, 1 lateral, 2 oblique, and 2 axial views. By applying these specific projections, we could visualize the epicondyles, the trochlea with its medial and lateral borders, the capitellum, the olecranon, the greater sigmoid notch, the coronoid process including its anteromedial facet, the proximal radioulnar joint with the radial tuberosity, and the anterior and posterior joint lines of the distal part of the humerus. These standard projections were reliably obtained using a specific sequence.

Conclusions: Knowledge about radiographic anatomy and standard projections is essential for visualizing important landmarks. With the presented standard projections of the elbow, important anatomical landmarks can be clearly examined. Thus, fluoroscopic visualization of anatomical fracture reduction and correct implant placement should be facilitated.

Clinical Relevance: This basic science cadaveric study defines fluoroscopic standard projections of the elbow essential for visualization of anatomical landmarks during surgery.

The radiohumeral, ulnohumeral, and proximal radioulnar joints of the elbow form a complex 3-dimensional (3D) structure. Standard radiographic views have been defined for anteroposterior (AP), lateral, and oblique planes, particularly for the radial head as described by Greenspan and Norman[1]. Additional oblique and axial views of the distal part of the humerus, the olecranon, and the coronoid have been characterized[2,3]. In the era of computed tomography (CT), however, radiography beyond the AP, lateral, and oblique views of the radial head[1] is rarely performed in clinical practice[4,5].

Even with the availability of new 3D technologies[6-11], intraoperative 2-dimensional (2D) fluoroscopy remains the standard imaging modality during surgery[8-10]. Fluoroscopy, however, may frequently fail to detect suboptimal positioning of implants and joint incongruities in the elbow[6,8] or in other joints[6,7,9,11]. Hence, 3D imaging has been advocated for complicated fractures in complex joints, such as ankle and calcaneal fractures. In contrast, no extra benefit from using intraoperative 3D imaging was found in the treatment of wrist fractures[11,12], and intraoperative 3D imaging appears to be less accurate than postoperative CT[7]. The published evidence on intraoperative 3D imaging of the elbow reporting superiority compared with 2D fluoroscopy is based on a total of 39 cases[6,8]. Moreover, the perceived superiority of 3D imaging may be due to a lack of knowledge regarding the interpretation of standard fluoroscopic projections. Clear guidance on intraoperative fluoroscopic standard positions of the elbow is

Fig. 1

The setup with the C-arm oriented perpendicular to the cadaver from the side of interest and the monitors on the contralateral side.

lacking. It may seem obvious to orthopaedic surgeons that, for instance, AP views should be made perpendicular to the radius and ulna[13], whereas lateral views would best be obtained by positioning the radiocapitellar joint parallel to the beam[14]. However, the utility of these positions has, to our knowledge, not been analyzed in detail. Therefore, the aim of the current cadaveric study was to confirm standard fluoroscopic AP and lateral views of the elbow and define new projections beyond the standard planes in order to visualize important anatomical landmarks for surgery.

Materials and Methods

Twelve cadaveric elbows were used for this study, which was divided into 2 parts. In part I, 6 elbows from the middle of the humerus to the middle of the forearm were studied under fluoroscopy for anatomical landmarks. In part II, findings from part I were confirmed using 6 elbows of 3 entire cadavers to mimic the intraoperative setting.

Specimens

Specimens were obtained from deceased donors who had voluntarily consented to the contribution of their body for science and research according to the regulations of the institutional department of anatomy. Cadavers had been embalmed using the Thiel technique[15], which has the advantage of preserving the flexibility of joints compared with formalin embalming[16]. Moreover, cadavers are preserved for later testing and handling is easier than with fresh-frozen cadavers, which need to be thawed for testing. Only for part I, all soft tissue was removed from the elbows, with the exception of the joint capsule and the medial and lateral ligaments. For part II, the elbows were not dissected and remained attached to the entire cadaver.

Fluoroscopy

For all assessments, a standard fluoroscopic C-arm (BV Endura; Philips) was used, and personal protection was worn according to institutional regulations.

Part I: Elbow Testing

The dissected elbows were imaged fluoroscopically by the most experienced authors (L.A. and D.R.). AP, lateral, oblique, and axial views were assessed for specific anatomical landmarks. The elbows were freely moved, rotated, and flexed during testing. Landmarks were projected freely whenever possible to eliminate the overlap of adjacent structures. In the case of ambiguity, landmarks were identified with a wire to specifically detect these areas under fluoroscopy. Part I resulted in several settings for different views of the elbow, which are described in detail within the Results section.

Part II: Simulated Intraoperative Positioning

After defining the standard projections and anatomical landmarks seen on the elbows utilized in part I, the equivalent standard projections were applied to the elbows of entire cadavers in a supine position with the shoulder at 90° of abduction. The C-arm was placed at a 90° angle to the cadaver on the same side as the tested elbow (Fig. 1). The beam was aligned vertically, extending from the floor toward the ceiling for all positions except the axial forearm view, which is described in detail in the Results section. Due to its common use, the term *anteroposterior* was used despite the actual *posteroanterior* direction of the beam. The positioning required to reproduce these projections regarding axial and rotational positions of the humerus and forearm as well as elbow flexion and extension were noted using a goniometer. A standardized sequence was defined to obtain all views that could be applied in an intraoperative setting. The defined sequence was
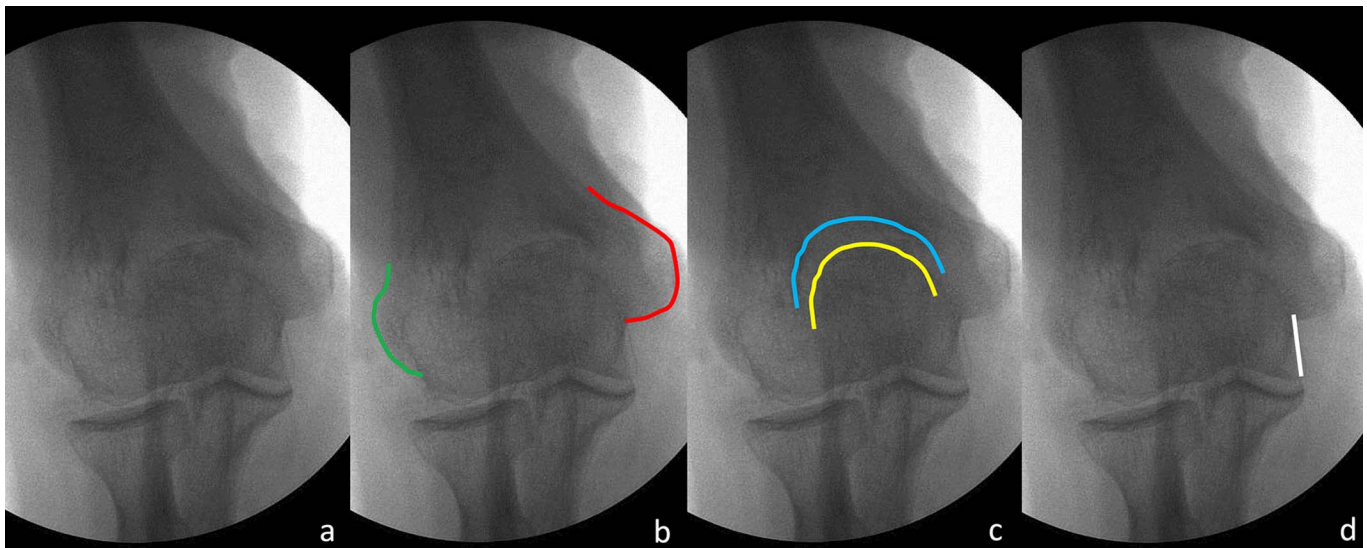
Fig. 2

Fig. 2-A Anteroposterior (AP) view of the distal part of the humerus. **Fig. 2-B** The medial (red line) and lateral (green line) epicondyles define the medial and lateral borders of the distal part of the humerus. **Fig. 2-C** The olecranon (yellow line) is centered within the olecranon fossa (blue line). **Fig. 2-D** The anterior and posterior contours of the medial edge of the trochlea are in alignment (white line), which is not the case on the lateral side.

tested by 3 investigators (S.A.M., C.B., and D.R.) for all samples in part II.

Results

Part I: Elbow Testing

Anteroposterior (AP) Views

Three AP views of the elbow were defined, focusing on the distal part of the humerus, the proximal part of the forearm, and the proximal radioulnar joint.

Aspects of the distal part of the humerus were best seen with the beam perpendicular to the transcondylar plane and with the elbow slightly flexed. Similarly, the proximal part of the forearm was best seen with the beam perpendicular to the supinated forearm. These 2 AP projections revealed different aspects to that observed in, for example, a single AP radiograph of the elbow. Obtaining these AP views for a flexed elbow facilitates imaging in traumatized elbows, in which a full extension may not be achieved.

In the AP view of the distal part of the humerus (Fig. 2), the epicondyles define the medial and lateral borders of the distal part of the humerus. The contour of the olecranon fossa is visible, with the olecranon centered, and the anterior and posterior contours of the medial edge of the trochlea are in alignment.

In the proximal forearm AP view (Fig. 3), the ulno-humeral joint lines are parallel medially and may diverge slightly
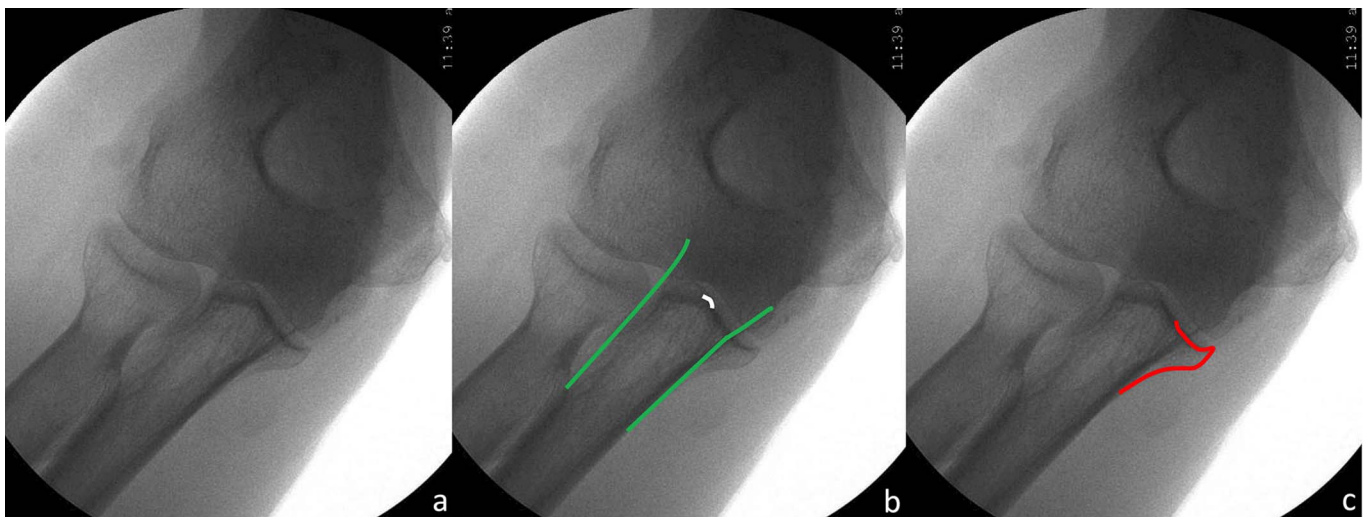

Fig. 3

Fig. 3-A Anteroposterior (AP) view of the proximal part of the forearm. **Fig. 3-B** The tip of the coronoid (short white line) is in the center of the proximal shaft of the ulna (green lines). **Fig. 3-C** The anteromedial facet of the coronoid (red line) is visible.
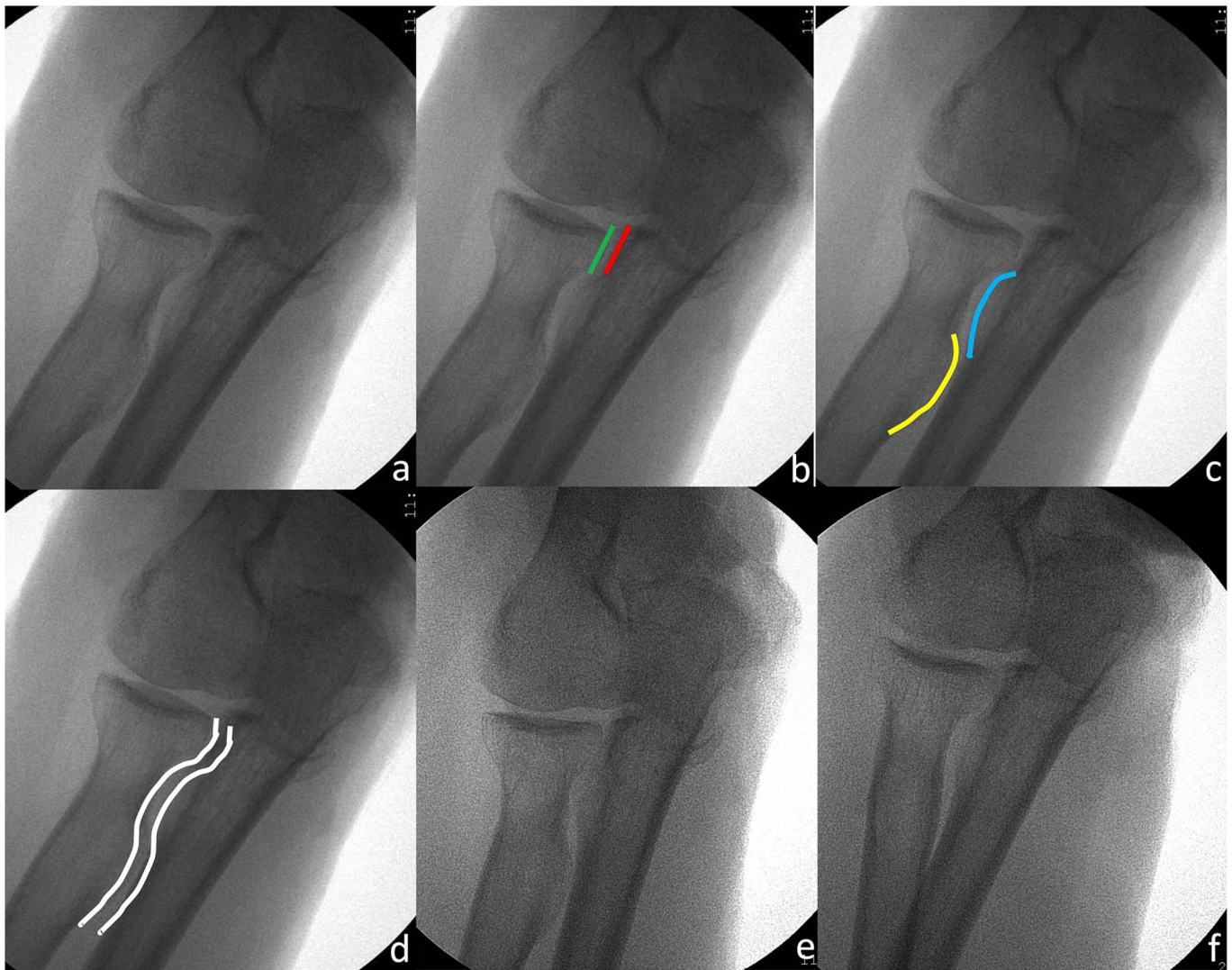
Fig. 4

Fig. 4-A View of the proximal radioulnar joint (PRUJ). **Fig. 4-B** The PRUJ is free from any overlap of the radial head (green line) and the lesser sigmoid notch (red line). **Fig. 4-C** The radial tuberosity (yellow line) and the supinator crest of the ulna (blue line) are visible, together forming a curvilinear shape (white lines, **Fig. 4-D**). Under constant fluoroscopy, the radial head can be examined from supination (**Fig. 4-E**) to pronation (**Fig. 4-F**).

laterally. The tip of the coronoid is in the midline of the proximal part of the ulna, and the anteromedial facet of the coronoid can be clearly seen.

In order to distinguish the proximal radioulnar joint (PRUJ) view (Fig. 4), the ulna—and thus the elbow—needs to be rotated externally about 30°, so that the lesser sigmoid notch is in line with the beam. In this projection, the supinator crest and the radial tuberosity are seen. The radial head can be evaluated throughout the full arc of forearm rotation.

Lateral View

Only 1 lateral view of the elbow was found optimal (Fig. 5). The elbow is flexed to 90°, the upper arm and forearm are perpendicular to the beam, and the forearm is in neutral rotation. The coronoid and radial head are projected in line as are the anterior aspect of the trochlea and capitellum, such that the anterior joint space is free without overlap of bones (Figs. 5-A, 5-B, and 5-C). In contrast, the posterior joint space cannot be cleared because of the overlap of the greater sigmoid notch and the posterior trochlea (Fig. 5-D). The most posterior structure is not the medial epicondyle but the lateral edge of the trochlea continuing to the posterior edge of the lateral column proximally (Fig. 5-E). The anterior border of the distal part of the humerus intersects the circle of the trochlea distally (Fig. 5-F). The center of the radial shaft is directed toward the center of the capitellum (Fig. 5-G). Finally, the proximal ulnar dorsal angulation, which is 5.7° (0° to 14°), on average[17], can be seen on the lateral view (Fig. 5-H).

Oblique Views

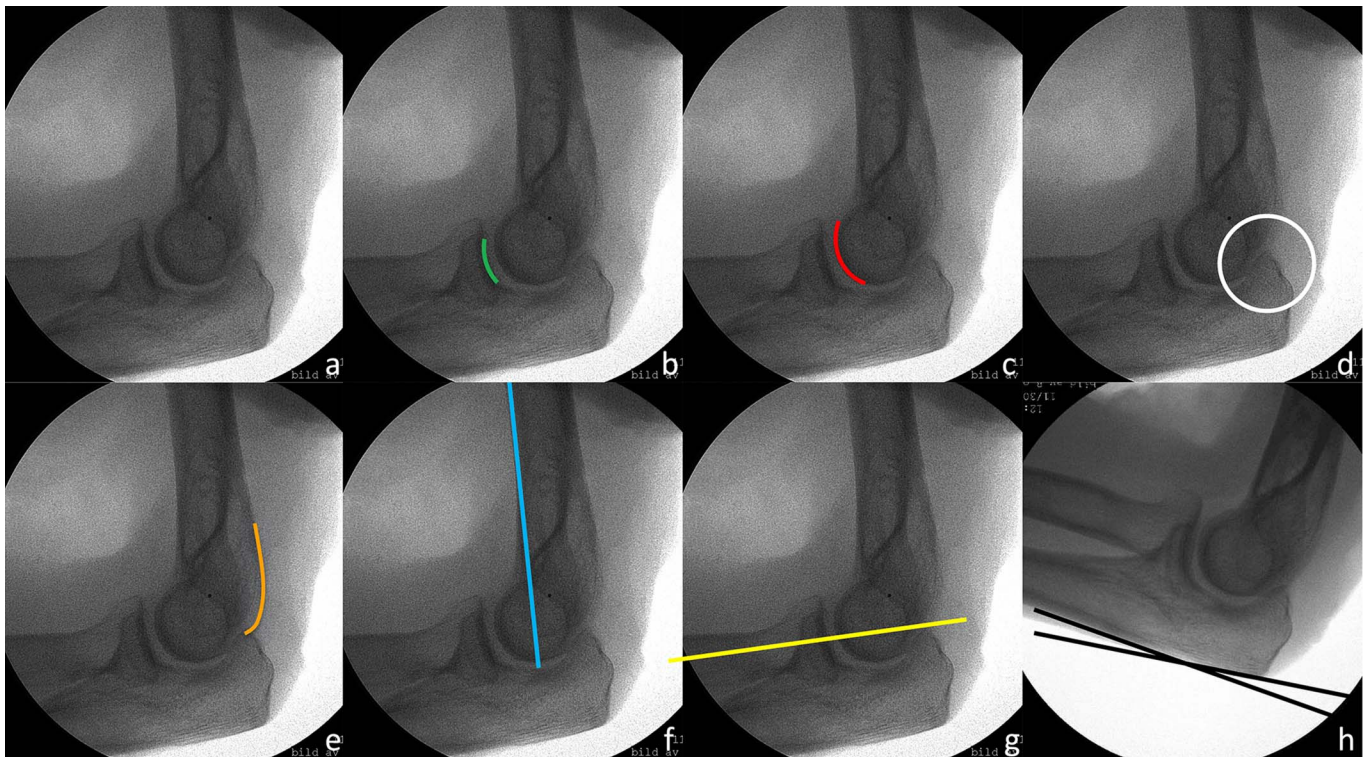By rotating the elbow, 2 distinctive oblique views were obtained:

Fig. 5

Fig. 5-A Lateral view of the elbow. **Fig. 5-B** The coronoid and radial head (green line) are projected in line, as are the trochlea and capitellum (red line, **Fig. 5-C**) without overlap of bones in the anterior joint. **Fig. 5-D** The posterior joint space cannot be visualized without overlap (white circle). **Fig. 5-E** The most posterior part of the distal aspect of the humerus in the lateral view is the posterior edge of the lateral column (orange line). **Fig. 5-F** Intersection of the trochlear circle with a line along the anterior border of the humerus (blue line). **Fig. 5-G** The radial shaft is centered toward the capitellum (yellow line). **Fig. 5-H** The black lines indicate the proximal ulnar dorsal angulation.

In 45° of external rotation, the "3-circle view" (Fig. 6) shows 3 semilunate lines, which indicate the ulnar and radial anterior borders of the trochlea as well as the contour of the capitellum. The greater sigmoid notch and the radial head together form a long curvilinear contour underneath.

By rotating the elbow 30° internally, the anteromedial facet of the coronoid and the greater sigmoid notch (anteromedial coronoid and olecranon view [Fig. 7]) were visualized.

With this projection however, the anteromedial facet with the sublime tubercle was better seen in flexion (Figs. 7-A and 7-B), whereas the tip of the coronoid was best visualized in extension (Figs. 7-C and 7-D).

Axial Views

In keeping with standard radiographic projections[3], 2 fluoroscopic axial views of the elbow were found (Fig. 8):

Fig. 6

Fig. 6-A Oblique 3-circle view of the elbow. The capitellum (green line) and the anterior radial (white line) and anterior ulnar (red line) borders of the trochlea on a fluoroscopic image (**Fig. 6-B**) and on anteroposterior (AP) and oblique artificial bone views for better visualization (**Fig. 6-C**).
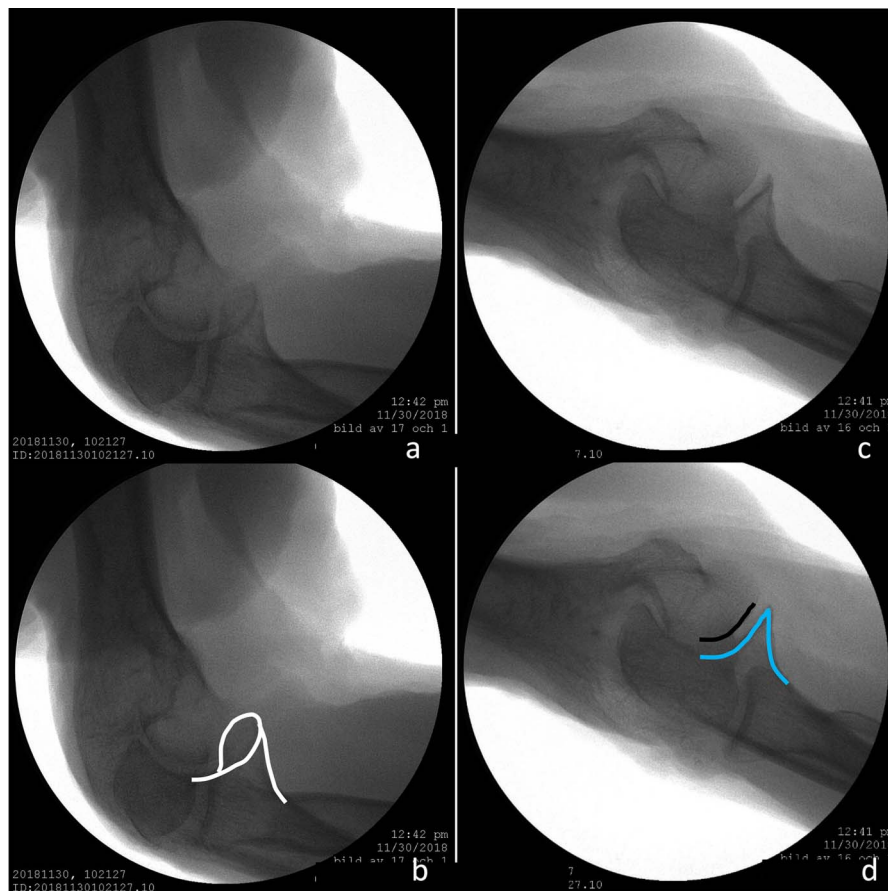
Fig. 7

Anteromedial coronoid and olecranon views in flexion (**Figs. 7-A and 7-B**) and extension (**Figs. 7-C and 7-D**). The anteromedial facet with the sublime tubercle is marked with a white line (**Fig. 7-B**) and is better seen in flexion. In extension, the tip of the coronoid is seen best (blue line, **Fig. 7-D**), as is the ulnar part of trochlea (black line, **Fig. 7-D**).

The axial humeral view involves positioning of the distal part of the humerus parallel to the image intensifier in a completely flexed elbow. The olecranon, the distal aspect of ulnohumeral joint, and the capitellum are seen.

The axial forearm view requires the elbow in the same position, but with the forearm parallel to the image intensifier. The anterior and posterior aspects of the trochlea as well as the capitellum are shown.

Part II: Simulated Intraoperative Positioning

Views from part I were confirmed using entire cadavers in a defined sequence, which had a reproducibility among the 3 investigators of 100%. This sequence is presented below.

(1) Distal Humeral AP View

The humerus is placed parallel to the floor and image intensifier and then rotated so that both epicondyles are visible and the olecranon tip is centered within the olecranon fossa. The elbow is slightly flexed and the forearm supinated (Fig. 9-A).

(2) Proximal Forearm AP View

From position 1, the forearm is lowered, the elbow flexed about 20° to 30°, and the supinated forearm is placed parallel to the floor and image intensifier (Fig. 9-B). The tip of the coronoid is in the center of the ulnar shaft and both the ulno- and radio-humeral joints are cleared.

(3) PRUJ View

From position 2, the ulna is kept parallel to the floor and image intensifier and externally rotated 30° to ensure that the PRUJ is projected freely along the lesser sigmoid notch without any overlap of bones (Fig. 9-C).

(4) 3-Circle View

From position 3, the elbow is rotated externally another 15° until the 3 semilunate circles of the ulnar and radial borders of the anterior aspect of the trochlea and coronoid are visible (Fig. 9-D).

(5) Anteromedial Coronoid and Olecranon View

Starting from position 2, the elbow is internally rotated 30° and flexed 70° (Fig. 9-E) so that the entire olecranon and coronoid
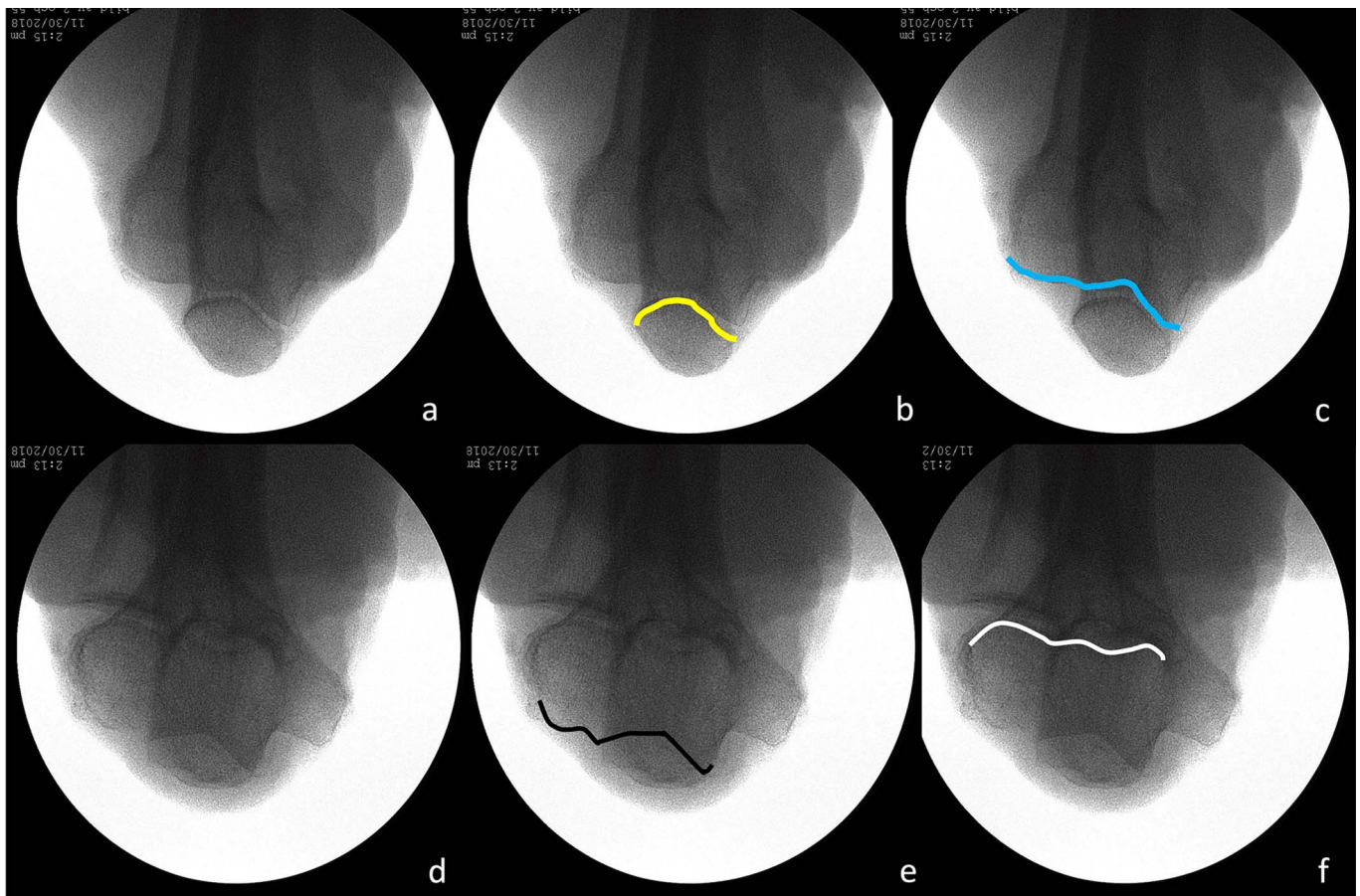
Fig. 8

Figs. 8-A, 8-B, and 8-C Axial humeral view. The olecranon (yellow line, **Fig. 8-B**) and the distal humeral joint line including the capitellum (blue line, **Fig. 8-C**) are visible. **Figs. 8-D, 8-E, and 8-F** Axial forearm view with the posterior (black line, **Fig. 8-E**) and anterior aspects of the trochlea as well as the capitellum (white line, **Fig. 8-F**) are visible.

with its anteromedial facet are visible. With greater extension, the ulnohumeral joint with the tip of the coronoid and ulnar part of the trochlea are visualized. Note that the anteromedial facet of the coronoid is only visible with more flexion.

(6) Lateral View

The best position for this view of the elbow depends on the amount of internal or external rotation that can be achieved by the patient's shoulder. The elbow is flexed 90°, the forearm is in neutral rotation, and the humerus is kept parallel to the floor and fluoroscope. The humerus is then either externally rotated 100° to 110° (Fig. 9-F) or internally rotated 70° to 80°, depending on how much the shoulder can be rotated. This allows the C-arm to remain in the same position as before. If there is limited rotation of the shoulder, the C-arm must be adjusted accordingly. With an ulnoradial projection, the radial head appears smaller and the coronoid larger, and vice versa with a radioulnar projection.

(7) Axial Humeral View

Starting with position 1, the elbow is fully flexed. The beam is aimed perpendicular to the humerus (Fig. 9-G).

(8) Axial Forearm View

The elbow is kept in position 7, and the C-arm is rotated so that the beam is perpendicular to the forearm (Fig. 9-H). Note that the position of the C-arm remains unchanged for positions 1 to 7 unless the lateral view (position 6) requires adjustment because of limited rotation of the patient's shoulder.

Discussion

The most important findings of this study were 8 different fluoroscopic views of the elbow showing important anatomical landmarks of the distal part of the humerus and the proximal part of the forearm. All presented views were reproducibly obtained using a specific sequence. This sequence may be modified as necessary based on the intraoperative circumstances; for instance, distal humeral pathology may be of greater interest than that of the proximal part of the forearm or vice versa.

While treating fractures, sufficient reduction to ultimately achieve the correct anatomy, i.e., the proximal ulnar dorsal angulation, and restoration of the trochlea or coronoid can be visualized optimally with the correct projection. In distal humeral fractures, the presented 3-circle view may be altered.

Fig. 9

Setups for the acquisition of different views. **Fig. 9-A** Distal humeral anteroposterior (AP) view (position 1): the humerus and image intensifier are parallel. The elbow is slightly flexed and the forearm supinated. **Fig. 9-B** Proximal forearm AP view (position 2): the forearm and image intensifier are parallel. From position 1, the forearm is lowered and the elbow is flexed 20° to 30°. **Fig. 9-C** The PRUJ view (position 3): from position 2, the forearm is kept parallel to the image intensifier and externally rotated 30°. **Fig. 9-D** The 3-circle view (position 4): from position 3, the elbow is externally rotated another 15°. **Fig. 9-E** Anteromedial coronoid and olecranon view (position 5): from position 2, the elbow is internally rotated 30° and flexed 70°. The more the elbow is extended, the less the anteromedial facet is visible and the more the ulnohumeral joint is cleared. **Fig. 9-F** Lateral view (position 6): the humerus is parallel to the image intensifier, and the elbow is flexed 90°. In this case, the shoulder is externally rotated 105° to obtain a true lateral view. **Fig. 9-G** Axial humeral view (position 7): From position 1, the elbow is fully flexed, and the beam is aimed perpendicular to the humerus. **Fig. 9-H** Axial forearm view (position 8): the same position of the elbow as position 7, with the beam aligned perpendicular to the forearm.

Restoration of the 3 circles may indicate correct repositioning. Treating radial head fractures, the PRUJ should be cleared and the radial head evaluated throughout pronation and supination. Thus, intra-articular screw penetration may be detected if anatomical landmarks are visualized in a standardized fashion. Particularly in the PRUJ, the presented protocol may also be used outside of the operating room to perform a dynamic evaluation with some additional information compared with static 3D imaging, such as CT or magnetic resonance imaging.

Standard 2D fluoroscopy remains the gold-standard imaging modality during surgery, as it is quick and easy. Consequently, standard projections need to be defined for reproducibility. For the elbow, there is a lack of consensus on the standard projections required to fluoroscopically assess this joint. For instance, over-lengthening of a radial head replacement has been studied on AP radiographs[18] and fluoroscopic scans[19] without describing the exact acquisition of an ideal AP view. In other cadaveric studies on the correct lengthening of a radial head replacement, true AP views of the radial head were defined with the beam perpendicular to the forearm, while the radial tuberosity could also be seen if the forearm was rotated externally[13,20]. Other studies used the lateral view to test for posterolateral rotatory instability[21] or placement

of a hinged external fixator[22] with a limited definition of a lateral view. Fluoroscopy of the elbow is also recommended for complete examination of the elbow without clear guidance on how to perform it[23]. To the best of our knowledge, this is the first study defining fluoroscopic standard views of the elbow.

Three-dimensional imaging has revolutionized diagnostics in clinical practice[6,11], and many operating rooms are now equipped with modern 3D imaging devices. However, 3D imaging is time-consuming[8,10] and radiation-intensive[24], and keeping the operating field sterile is cumbersome as devices need to be rotated around the center of interest. Evidence suggesting the superiority of intraoperative 3D imaging of elbow trauma is limited. In complex elbow trauma, intraoperative 3D imaging was shown to detect more incongruities and implant malpositioning compared with fluoroscopic AP and lateral views[8]. However, in that case series of 36 patients, neither the acquisition of fluoroscopic AP or lateral views was defined nor were additional views beyond AP or lateral obtained. Thus, it might be questioned whether the results would have differed with the knowledge and use of the presented 8 fluoroscopic views of the elbow.

The complex 3D anatomy of the elbow adds to the intricacy of achieving correct positioning of both the elbow and the 2D imaging device, which is why defined views are needed. Such views have already been defined for the wrist. These views include AP, lateral, oblique, and axial, such as the "skyline view" or the "carpal shoot-through view," and are routinely used[25-30]. The knowledge of distinct fluoroscopic views of the wrist may be the reason why 3D imaging does not appear to have an additional benefit in the treatment of wrist fractures compared with 2D fluoroscopy[11,12].

There were limitations to the current study. First, this was a cadaveric and not a clinical study. Fluoroscopic views were tested under ideal laboratory conditions using dissected elbows as well as entire cadavers, aiming for a realistic intraoperative setting. Despite reproducible results in this testing environment, confirmation of the presented views in the true operative setting is needed. Second, imaging was only tested in a supine position. Some elbow surgeries require a lateral or prone position. Fluoroscopic views for these positions should be obtainable by adjusting the C-arm accordingly. Third, outlining anatomical landmarks does not necessarily mean that malpositioning of implants or incorrect fracture reduction is depicted, as this has not been investigated. Standard projections and their reliable acquisition need to be defined first, which was the actual aim of this study. Last, the radiation dosage was not recorded during testing. However, once the algorithm had been defined, the presented views were obtained quickly and reliably, resulting in limited radiation exposure. Further clinical studies are needed to validate the defined standard projections during surgery and compare those with intraoperative 3D imaging.

This study presents a clear algorithm for fluoroscopic imaging of the anatomy of the elbow. Intraoperative fluoroscopy may guide the clinician during surgery, when applied as described. The ability to obtain standardized views and knowledge of the radiographic anatomy may help to improve both fracture reduction and implant placement. ∎

Sebastian A. Müller, MD[1]
Lars Adolfsson, MD[2]
Cornelia Baum, MD[1]
Magdalena Müller-Gerbl, MD[1]
Andreas M. Müller, MD[1]
Daniel Rikli, MD[1]

[1]Department of Orthopedic Surgery (S.A.M., C.B., A.M.M., and D.R.) and Institute of Anatomy (M.M.-G.), University of Basel, Basel, Switzerland

[2]Department of Orthopedic Surgery, Linköping University, Linköping, Sweden

ORCID iD for S.A. Müller: 0000-0001-8183-8080
ORCID iD for L. Adolfsson: 0000-0001-7873-3093
ORCID iD for C. Baum: 0000-0002-3813-6742
ORCID iD for M. Müller-Gerbl: 0000-0002-4875-1685
ORCID iD for A.M. Müller: 0000-0003-2726-3428
ORCID iD for D. Rikli: 0000-0002-0999-4588

References

1. Greenspan A, Norman A. The radial head, capitellum view: useful technique in elbow trauma. AJR Am J Roentgenol. 1982 Jun;138(6):1186-8.

2. Gottschalk HP, Bastrom TP, Edmonds EW. Reliability of internal oblique elbow radiographs for measuring displacement of medial epicondyle humerus fractures: a cadaveric study. J Pediatr Orthop. 2013 Jan;33(1):26-31.

3. Souder CD, Farnsworth CL, McNeil NP, Bomar JD, Edmonds EW. The distal humerus axial view: assessment of displacement in medial epicondyle fractures. J Pediatr Orthop. 2015 Jul-Aug;35(5):449-54.

4. Edmonds EW. How displaced are "nondisplaced" fractures of the medial humeral epicondyle in children? Results of a three-dimensional computed tomography analysis. J Bone Joint Surg Am. 2010 Dec 1;92(17):2785-91.

5. Singson RD, Feldman F, Rosenberg ZS. Elbow joint: assessment with double-contrast CT arthrography. Radiology. 1986 Jul;160(1):167-73.

6. Carelsen B, Haverlag R, Ubbink DT, Luitse JS, Goslings JC. Does intraoperative fluoroscopic 3D imaging provide extra information for fracture surgery? Arch Orthop Trauma Surg. 2008 Dec;128(12):1419-24. Epub 2008 Sep 13.

7. Kendoff D, Citak M, Gardner MJ, Stübig T, Krettek C, Hüfner T. Intraoperative 3D imaging: value and consequences in 248 cases. J Trauma. 2009 Jan;66(1):232-8.

8. Schnetzke M, Fuchs J, Vetter SY, Beisemann N, Keil H, Grützner PA, Franke J. Intraoperative 3D imaging in the treatment of elbow fractures—a retrospective analysis of indications, intraoperative revision rates, and implications in 36 cases. BMC Med Imaging. 2016 Mar 18;16:24.

9. Franke J, von Recum J, Wendl K, Grützner PA. [Intraoperative 3-dimensional imaging - beneficial or necessary?]. Unfallchirurg. 2013 Feb;116(2):185-90. German.

10. Atesok K, Finkelstein J, Khoury A, Peyser A, Weil Y, Liebergall M, Mosheiff R. The use of intraoperative three-dimensional imaging (ISO-C-3D) in fixation of intra-articular fractures. Injury. 2007 Oct;38(10):1163-9. Epub 2007 Sep 19.

11. Beerekamp MS, Sulkers GS, Ubbink DT, Maas M, Schep NW, Goslings JC. Accuracy and consequences of 3D-fluoroscopy in upper and lower extremity fracture treatment: a systematic review. Eur J Radiol. 2012 Dec;81(12):4019-28. Epub 2012 Sep 10.

12. Wirth S, Euler E, Kotsianos-Hermle D, Treitl M, Linsenmaier U, Pfeifer KJ, Reiser M, Mutschler W. [Comparison of C-arm CT and standard imaging in osteosyntheses

of fractured distal radius specimens]. Unfallchirurg. 2007 Jan;110(1):41-8. German.

13. Kim HM, Roush EP, Kiser C. Intraoperative fluoroscopic assessment of proper prosthetic radial head height. J Shoulder Elbow Surg. 2016 Nov;25(11):1874-81. Epub 2016 Jun 27.

14. Rastogi AK, Davis KW, Ross A, Rosas HG. Fundamentals of joint injection. AJR Am J Roentgenol. 2016 Sep;207(3):484-94. Epub 2016 Jun 8.

15. Thiel W. [The preservation of the whole corpse with natural color]. Ann Anat. 1992 Jun;174(3):185-95. German.

16. Eisma R, Lamb C, Soames RW. From formalin to Thiel embalming: what changes? One anatomy department's experiences. Clin Anat. 2013 Jul;26(5):564-71. Epub 2013 Feb 13.

17. Rouleau DM, Faber KJ, Athwal GS. The proximal ulna dorsal angulation: a radiographic study. J Shoulder Elbow Surg. 2010 Jan;19(1):26-30.

18. Athwal GS, Rouleau DM, MacDermid JC, King GJ. Contralateral elbow radiographs can reliably diagnose radial head implant overlengthening. J Bone Joint Surg Am. 2011 Jul 20;93(14):1339-46.

19. Schnetzke M, Feuchtenhofer F, Keil H, Swartman B, Vetter S, Grützner PA, Franke J. Radiographic assessment of overlengthening of the MoPyC radial head prosthesis: a cadaveric study. Arch Orthop Trauma Surg. 2019 Nov;139(11):1543-9. Epub 2019 Apr 13.

20. Shukla DR, Vanhees MKD, Fitzsimmons JS, An KN, O'Driscoll SW. Validation of a simple overlay device to assess radial head implant length. J Hand Surg Am. 2018 Dec;43(12):113510.e1-8. Epub 2018 Jun 8.

21. Camp CL, Smith J, O'Driscoll SW. Posterolateral rotatory instability of the elbow: part II. Supplementary examination and dynamic imaging techniques. Arthrosc Tech. 2017 Apr 3;6(2):e407-11.

22. Wiggers JK, Snijders RM, Dobbe JGG, Streekstra GJ, den Hartog D, Schep NWL. Accuracy in identifying the elbow rotation axis on simulated fluoroscopic images

using a new anatomical landmark. Strategies Trauma Limb Reconstr. 2017 Nov; 12(3):133-9. Epub 2017 Jun 7.

23. Hausman MR, Lang P. Examination of the elbow: current concepts. J Hand Surg Am. 2014 Dec;39(12):2534-41. Epub 2014 Nov 21.

24. Mehling I, Rittstieg P, Mehling AP, Küchle R, Müller LP, Rommens PM. Intraoperative C-arm CT imaging in angular stable plate osteosynthesis of distal radius fractures. J Hand Surg Eur Vol. 2013 Sep;38(7):751-7. Epub 2013 Feb 6.

25. Dolce D, Goodwin D, Ludwig M, Edwards S. Intraoperative evaluation of dorsal screw prominence after polyaxial volar plate fixation of distal radius fractures utilizing the Hoya view: a cadaveric study. Hand (N Y). 2014 Dec;9(4):511-5.

26. Marsland D, Hobbs CM, Sauvé PS. Volar locking plate fixation of distal radius fractures: use of an intra-operative 'carpal shoot through' view to identify dorsal compartment and distal radioulnar joint screw penetration. Hand (N Y). 2014 Dec;9(4):516-21.

27. Matullo KS, Dennison DG. Lateral tilt wrist radiograph using the contralateral hand to position the wrist after volar plating of distal radius fractures. J Hand Surg Am. 2010 Jun;35(6):900-4. Epub 2010 May 15.

28. Ozer K, Wolf JM, Watkins B, Hak DJ. Comparison of 4 fluoroscopic views for dorsal cortex screw penetration after volar plating of the distal radius. J Hand Surg Am. 2012 May;37(5):963-7. Epub 2012 Apr 4.

29. Riddick AP, Hickey B, White SP. Accuracy of the skyline view for detecting dorsal cortical penetration during volar distal radius fixation. J Hand Surg Eur Vol. 2012 Jun; 37(5):407-11. Epub 2011 Nov 7.

30. Stoops TK, Santoni BG, Clark NM, Bauer AA, Shoji C, Schwartz-Fernandes F. Sensitivity and specificity of skyline and carpal shoot-through fluoroscopic views of volar plate fixation of the distal radius: a cadaveric investigation of dorsal cortex screw penetration. Hand (N Y). 2017 Nov;12(6):551-6. Epub 2016 Nov 1.